ELSEVIER

Coordination Chemistry Reviews 237 (2003) 213–228

COORDINATION CHEMISTRY REVIEWS

www.elsevier.com/locate/ccr

Oxovanadium(III–V) mononuclear complexes and their linear assemblies bearing tetradentate Schiff base ligands: structure and reactivity as multielectron redox catalysts

Eishun Tsuchida *, Kenichi Oyaizu

Advanced Research Institute for Science and Engineering, Waseda University, Tokyo 169-8555, Japan

Received 25 January 2002; accepted 5 September 2002

Contents

Abstract

This review summarizes the recent advances in the chemistry of oxovanadium(III–V) mononuclear complexes and their linear assemblies bearing tetradentate Schiff base ligands. Structural parameters of the oxovanadium assemblies are compiled, which reveal the preference of specific coordination geometries around vanadium atoms according to the valence state. Emphasis is placed on the catalysis of multielectron redox reactions by oxovanadium(IV) complexes which disproportionate to vanadium(III) and oxovanadium(V) complexes under suitable conditions. Their biological implications and synthetic applications are described.

Keywords: Oxovanadium complexes; Schiff base ligands; Crystal structures; Redox reaction; Catalysis

1. Introduction

The chemistry of vanadium(IV) is dominated by the stable oxovanadium (VO^{2+}) cation which remains intact during many reactions. The deoxygenation of oxovanadium(IV) complexes to form six-coordinate vanadium(IV) complexes usually enhances their reactivity. Since vanadium(V) is a strong oxidant and vana-

* Corresponding author. Tel.: +81-3-5286-3120; fax: +81-3-3205-4740

E-mail address: eishun@mn.waseda.ac.jp (E. Tsuchida).

0010-8545/02/$ - see front matter
PII: S0010-8545(02)00251-5

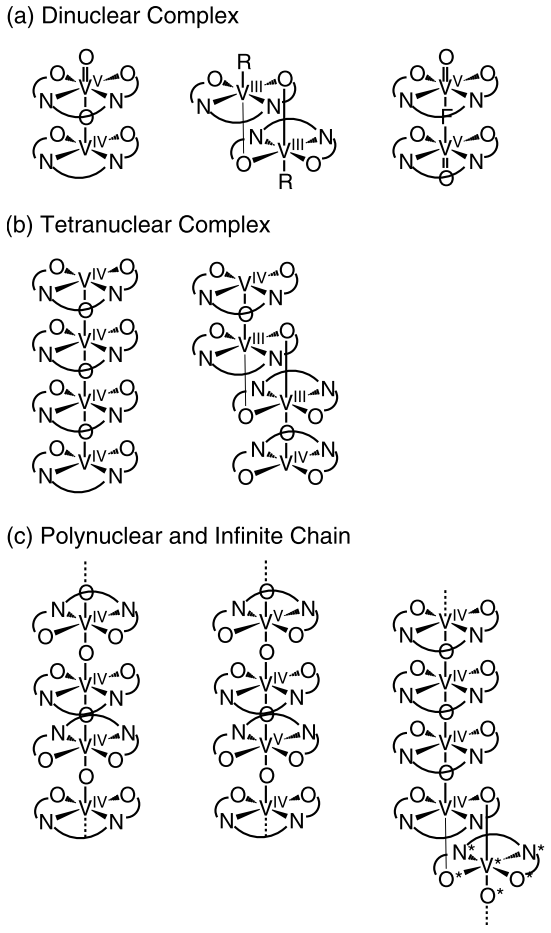

Scheme 1.

dium(III) can be oxidized by O_2, redox reactions including the V(IV)/V(III) and V(V)/V(IV) couples are of interest in relation to the autoxidation of organic molecules. This review summarizes the recent advances in the chemistry of oxovanadium(III–V) mononuclear complexes and their linear assemblies bearing tetradentate Schiff base ligands such as $salen^{2-}$ and $salptn^{2-}$. With tetradentate Schiff base ligands occupying the equatorial positions, the preference of vanadium(III) and vanadium(V) to be six-coordinate rather than five drives the formation of a variety of linear oxovanadium assemblies as shown in Scheme 1.

Structural parameters from the crystal data (static pictures) of the oxovanadium assemblies are compiled, which not only reveal the preference of specific coordination geometries around the vanadium atoms according to the valence state, but also provide important chemical reaction coordinates to represent the structural changes occurring in the V(IV)/V(III) and V(V)/V(IV) redox reactions.

The oxovanadium assemblies could persist in solutions or dissociate into mononucleic species. Recent interest has also been stimulated by their significance as multielectron redox catalysts. Emphasis is placed on the catalysis of multielectron redox reactions by oxovanadium(IV) complexes which disproportionate to vanadium(III) and oxovanadium(V) complexes under suitable conditions. Their biological implications and synthetic applications, in addition to the reactivity of mononuclear complexes associated with the formation of the assemblies, are summarized in this review.

2. O_2 splitting reactions by μ-oxo dinuclear complexes

The capacity of metalloenzymes to transduce energy via synergetic electron transfer for the assimilative reduction of small molecules such as CO_2 and N_2 and O_2-oxidations in dissimilatory processes poses a considerable challenge to modeling the biological processes. As one of the recent topics, the crystal structure of cytochrome *c* oxidases which provokes a four-electron reduction of O_2 to H_2O has attracted much attention [1] though the structures of the intermediate O_2 adducts or their catalytic mechanisms have not been realized in detail. As to the four-electron reduction system of O_2, much effort has been spent to establish an effective electrocatalyst that operates near the thermodynamic potential. On the other hand, much interest has also been directed toward the application of well-defined four-electron reduction systems of O_2 to molecular synthesis. Indeed, a number of important biological and industrial processes involve the metal-catalyzed oxidation of organic substrates, and for this purpose the use of O_2 as the ultimate oxidant has obvious advantages in terms of cost and handling use.

A novel synthetic route for poly(thio-1,4-phenylene), an important engineering plastic, has been established by the oxovanadium-catalyzed O_2-oxidative polymerization of diphenyl disulfide [2]. Bis(β-diketonato)oxovanadium(IV) complexes such as $[VO(acac)_2]$, $[VO(bzac)_2]$ and $[VO(tfac)_2]$ act as excellent catalysts in non-aqueous acidic media, but mechanistic analysis of the redox process involved in the catalytic cycle is difficult because of the lability of the β-diketone ligands [3]. The redox chemistry of a more stable model of the catalyst bearing tetradentate Schiff base ligands in place of the β-diketone ligands has been described, and this revealed that a μ-oxo divanadium(IV) complex $[LV^{IV}–O–LV^{IV}]^{2+}$ (L = ligand(−2)) is formed under strongly acidic non-aqueous conditions as the catalytically active species. Since the oxidative polymerization of diphenyl disulfide catalyzed by oxovanadium complexes results in a selective formation of thioether bonds without any oxygenated compounds such as sulfoxides and/or sul-

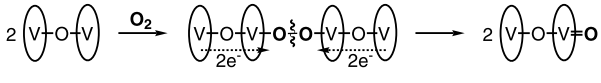

Scheme 2.

fones, H_2O should be produced predominantly by the four-electron reduction of O_2 catalyzed by the vanadium complex without the formation of partially-reduced side products such as H_2O_2. Central to the issue of this review is the novel O_2 splitting reactions with four electrons through the homolytic cleavage of μ-dioxo tetranuclear complexes (Scheme 2) involved in the catalysis of the μ-oxo divanadium complexes in the reduction of O_2 to H_2O.

The reactivity of vanadium complexes toward O_2 is responsive to the oxidation state and the coordination structure. A typical example has been provided by acetylacetonate complexes: a six-coordinate vanadium(III) complex $V(acac)_3$ is slowly oxidized by O_2 whereas a five-coordinate vanadium(IV) complex $VO(acac)_2$ is stable in air. On the other hand, a multielectron transfer process from the vanadium(III) complex to O_2 has also been reported, which not only reveals the O_2-oxidation mechanism of diphenyl disulfide but also provides additional insight into the unique chemistry of vanadium with possible relevance to metal monooxygenases. For the present, it may be useful to look more closely at some of the important features of the multielectron transfer from a vanadium(III) complex to O_2. It has been found that the oxidation of a μ-oxo divanadium(III, IV) complex $[LV^{IV}–O–LV^{III}]^+$ with O_2 in anhydrous CH_2Cl_2 proceeds almost stoichiometrically to produce $[LV^{IV}–O–LV^{V}=O]^+$ [4]. The typical complexes formulated as $[LV^{IV}–O–LV^{III}]^+$ and $[LV^{IV}–O–LV^{V}=O]^+$ have been isolated as single crystals and their structures have been determined (Fig. 1) [5].

The $[LV^{IV}–O–LV^{III}]^+$ and $[LV^{IV}–O–LV^{V}=O]^+$ cations persist in non-polar solvents such as CH_2Cl_2 but dissociate into mononuclear complexes in polar solvents

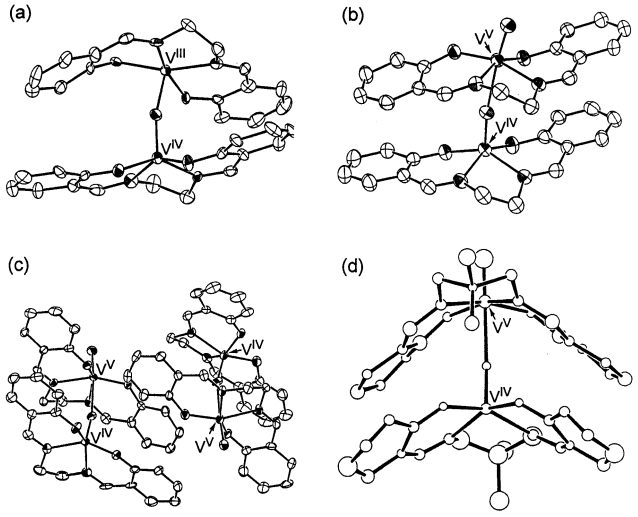

Fig. 1. Crystal structures of: (a) $[(salen)V^{IV}–O–V^{III}(salen)][I_3]$; (b) $[(salen)V^{IV}–O–V^{V}(salen)=O][ClO_4]$; (c) $[(salen)V^{IV}–O–V^{V}(salen)=O][I_3]$ (asymmetric unit); and (d) $[(salptn)V^{IV}–O–V^{V}(salptn)=O][I_3]$. Counter anions and hydrogen atoms are omitted for clarity.

$$[LV^{IV}\text{-}O\text{-}LV^{III}]^+ \longrightarrow [LV^{IV}{=}O] + [LV^{III}]^+$$

$$[LV^{IV}\text{-}O\text{-}LV^{V}{=}O]^+ \longrightarrow [LV^{IV}{=}O] + [LV^{V}{=}O]^+$$

Scheme 3.

$$[LV^{IV}\text{-}O\text{-}LV^{III}]^+ + \mathbf{O_2} \underset{k_{-1}}{\overset{k_1}{\rightleftharpoons}} [LV\text{-}O\text{-}LV\text{-}\mathbf{O_2}]^+$$

$$[LV\text{-}O\text{-}LV\text{-}\mathbf{O_2}]^+ + [LV\text{-}O\text{-}LV]^+ \xrightarrow{k_2} [LV^{IV}\text{-}O\text{-}LV^{IV}\text{-}\mathbf{O}\text{-}\mathbf{O}\text{-}LV^{IV}\text{-}O\text{-}LV^{IV}]^{2+}$$

$$[LV^{IV}\text{-}O\text{-}LV^{IV}\text{-}\mathbf{O}\text{-}\mathbf{O}\text{-}LV^{IV}\text{-}O\text{-}LV^{IV}]^{2+} \xrightarrow[\text{(fast)}]{k_3} 2\,[LV^{IV}\text{-}O\text{-}LV^{V}{=}\mathbf{O}]^+$$

Scheme 4.

such as CH_3CN and even in CH_2Cl_2 in the presence of supporting electrolytes (Scheme 3) [6]. In pure CH_2Cl_2, the oxidation of $[LV^{IV}–O–LV^{III}]^+$ with O_2 obeys a rate law second order with respect to $[LV^{IV}–O–LV^{III}]^+$ and first-order in O_2, which suggests a mechanism of oxidation involving a bimolecular reaction to produce an O_2-adduct, the μ-dioxo tetranuclear complex, as the rate limiting step [5]. The steady-state approximation to $[LV^{IV}–O–LV^{III}]^+$ and $[LV^{IV}–O–LV^{IV}–O–O–LV^{IV}–O–LV^{IV}]^{2+}$ yields the rate law $-d[LV^{IV}–O–LV^{III+}]/dt = 2k_1k_2[LV^{IV}–O–LV^{III+}]^2[O_2]/(k_{-1}+k_2[LV^{IV}–O–LV^{III+}])$. The second order dependence of the rate in $[LV^{IV}–O–LV^{III}]^+$ suggests that the release of O_2 from $[LV–O–LV–O_2]^+$ is fast ($k_{-1} > k_2[LV^{IV}–O–LV^{III+}]$) which is reflected in the slow rate of the overall reaction [4]. The homolytic scission of the intermediate is the likely reaction to generate two molecules of the $[LV^{IV}–O–LV^{V}=O]^+$ cation (Scheme 4).

Added support for the formation of the μ-dioxo tetranuclear complex has been provided by the isolation of the O_2 adduct at reduced temperatures. The vanadium mean oxidation state estimated by XANES experiments using standard samples, the Raman shift of the $^{16}O_2$ adduct and the isotope effect using $^{18}O_2$, are in accordance with the formation of the μ-dioxo tetravanadium(IV) complex $[LV^{IV}–O–LV^{IV}–O–O–LV^{IV}–O–LV^{IV}]^{2+}$ [7].

The stoichiometry of the O_2 splitting reaction (Scheme 2) is reminiscent of the electroreduction of O_2 to H_2O. It is of interest that oxygenation of vanadium(III) gives oxovanadium(V), whereas multiple redox centers have been considered to be essential for the incorporation of O_2. An explanation for this can be found in the reactivity of the five-coordinate vanadium(III) with O_2 and the stability of the resulting oxovanadium(V) complexes. A further important issue is the implication of vanadium(III)/oxovanadium(V) interconversion. O_2-oxidation of metal complexes to oxometal complexes ($LM^x + 1/2O_2 \rightarrow LM^{x+2}{=}O$) produces a fully reduced oxo ligand, and the resulting high-valent complexes often act as multielectron redox

catalysts [8]. In addition, a two-electron transfer process involved in the protonation-assisted interconversion between vanadium(III) and oxovanadium(V) might play a role in the operation of prosthetic groups mediating biological redox reactions such as those of the vanadium haloperoxidases [9] and in the unknown function of accumulated vanadium(III) in sea squirts [10]. The structures and the reactivity of mononuclear complexes and their assemblies provide the mechanism of the two-electron transfer that occur from both sides of the μ-oxo dinuclear complex to O_2 (vide infra).

3. Structures and reactivity

Electrochemical and structural studies of oxovanadium complexes with tetradentate Schiff base ligands attract particular attention because of their reversible one-electron redox behavior. Indeed, oxovanadium complexes with a large number of tetradentate Schiff base ligands have been reported. In general, they tend to form linear polymeric chains (···V=O···V=O···) in the solid state with Schiff base ligands bearing six-membered N–N chelate rings such as those derived from 1,3-propanediamine [11]. The preference of vanadium(V) and vanadium(III) to be six-coordinate rather than five drives the formation of mixed-valent assemblies. The deoxygenation of oxovanadium(IV) to oxophilic vanadium(IV) complexes could lead to the formation of multinuclear complexes bearing V–O–V bonds. Herein a number of recent studies on the structures and the reactivity of mononuclear complexes and μ-oxo multinuclear complexes are reviewed in order to derive not only the mechanism of V–O–V bond formation but also the redox-reaction coordinate associated with the O_2 splitting reaction by the μ-oxo dinuclear complexes as shown in Scheme 2.

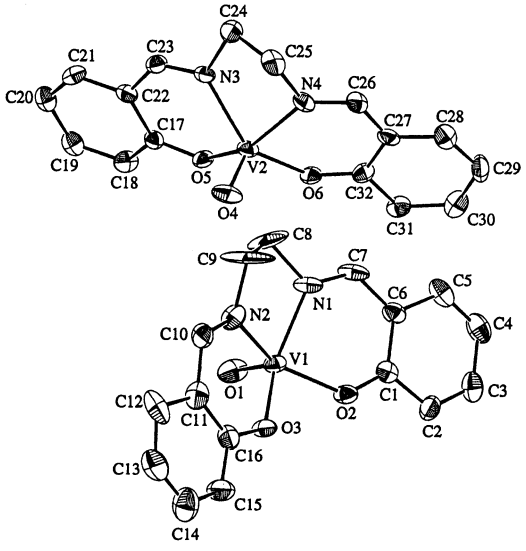

Fig. 2. ORTEP view of [VO(salen)] (30% probability ellipsoids) [13]: monoclinic space group $P2_1$ (#14), $a = 13.622(4)$, $b = 6.812(2)$, $c = 15.949(3)$ Å, $\beta = 98.18(2)^\circ$, $V = 1465.0(6)$ Å^3, $Z = 4$, $D_{calc} = 1.511$ g cm^{-3}, $\mu(\text{Mo–K}_\alpha) = 5.52$ cm^{-1}, $R = 0.063$, $R_w = 0.057$. Hydrogen atoms are omitted for clarity.

3.1. Mononuclear complexes

[V^{IV}O(salen)] crystallizes easily and their X-ray structures have been solved [12]. Polymorphism has been found in the crystal structure of [VO(salen)] [13] in which the asymmetric unit contains two independent molecules with minor conformational differences (Fig. 2).

Crystal structures of [VO(salen)] derivatives bearing a variety of substituents such as alkyl and alkoxyl groups [14] on the salicylideneimine moiety have been reported. These complexes typically adopt the square pyramidal coordination geometry around the vanadium(IV) center.

Square pyramidal to trigonal bipyramidal distortion of oxovanadium(IV) complexes with sterically crowded Schiff base ligands was originally studied by crystallographic and electron paramagnetic resonance analyses [15]. The pulsed electron paramagnetic resonance technique of ^{51}V electron spin echo-electron nuclear double resonance has also been used to measure the nuclear quadrupole coupling constants of a series of five-coordinate oxovanadium(IV) complexes containing Schiff base ligands with geometries ranging from distorted square pyramidal to distorted trigonal bipyramidal; vanadium nuclear quadrupole coupling constants have been found to be particularly sensitive to the coordination geometry of the oxovanadium ion, and thus sensitive to the structural distortions [16].

[VO(salen)] displays a variety of coordination chemistry in strongly acidic solution depending on the choice of solvent, the proton source, and the presence or absence of O_2. Under aerobic conditions, the addition of anhydrous HCl to the CH_3CN solution of [VO(salen)] results in the protonation and dissociation of the oxo group, providing [$V^{IV}Cl_2$(salen)] [17]. In contrast, when aqueous $HClO_4$ is added to the CH_3CN solution of [VO(salen)], [V^{V}O(salen)][ClO_4] is isolated which arises from a disproportionation of [VO(salen)] giving both [VO(salen)][ClO_4] and a vanadium(III) species that is oxidized to [VO(salen)][ClO_4] by O_2 [17]. The vanadium(III) species originally assumed to be $[V^{III}H_2(salen)]^{3+}$ [17] was determined to be $[V^{III}(salen)]^{+}$ [18] by titration experiments performed under strictly anhydrous conditions using CF_3SO_3H. The acid-induced disproportionation of [VO(salen)] is discussed later in this review.

The exchange reaction of the oxygen atom in H_2O with the oxo group bound to the vanadium(IV) center proceeds only slowly in DMSO under argon [19]. On the other hand, deoxygenation of oxovanadium(IV) Schiff base complexes by $SOCl_2$ efficiently gives the corre-

sponding dichlorovanadium(IV) derivatives according to $[VO(salen)]+SOCl_2 \rightarrow [VCl_2(salen)]+SO_2$ [20]. Alternatively, PCl_5 in benzene can effect the conversion of [VO(salen)] to $[VCl_2(salen)]$ [21]. Similarly, PPh_3Br_2 and [VO(salen)] yield $[VBr_2(salen)]$ [22]. Trimethylsilyl iodide has been found to be effective in the conversion of [VO(salen)] to $[VI_2(salen)]$ [23]. The reaction of $[VCl_2(salen)]$ with PhLi results in the replacement of the chloro groups by phenyl groups to produce $[VPh_2(salen)]\cdot CH_3OH$, an organovanadium(IV) compound which is thermally stable at room temperature [24]. The sulfur analogue of [VO(acen)], [VS(acen)], is formed by treating [VO(acen)] with B_2S_3 in rigorously dry CH_2Cl_2 [25]. The product is quite O_2 sensitive in solution and readily reverts back to [VO(acen)]. The thiovanadium(IV) complex [VS(salen)] has also been prepared by the reaction of [VO(salen)] with B_2S_3 [26]. Crystallographic studies of [VO(acen)] [27] show its structure to be a rectangular pyramid with the terminal oxygen atom at the apex. The structure of [VS(acen)] has also been reported [28] and is quite similar to that of [VO(acen)] except for the V=O and V=S bond lengths. The V=S bond (2.061 Å) is closer to a single bond in length.

Oxovanadium(IV) complexes with Schiff base ligands derived from *meso*-1,2-diphenyl-1,2-ethanediamine are dehydrogenated by heating at 210 °C for 3–15 h in the solid state to produce oxovanadium(IV) complexes with the corresponding Schiff base ligands containing 1,2-ethenediimine units; the benzylic carbon atoms of the N–N chelate ring are oxidized by O_2 to from a C=C double bond and H_2O ($[VO(Xsal\text{-}meso\text{-}stien)]+1/2O_2 \rightarrow [VO(Xsalton)]+H_2O$, where X = 5-bromo, 5-ethoxy or 3-ethoxy groups) [29]. An oxovanadium(IV) complex with ethylenebis[(*o*-hydroxyphenyl)glycine] as a ligand decomposes in DMF solution to produce VO(salen) [30]. This reaction corresponds to an oxidative decarboxylation in which two molecules of CO_2, three protons, and three electrons are lost to generate [VO(salen)] [12].

The reaction of [Cu(salen)] with $VOCl_2$ in $CHCl_3/C_2H_5OH$ mixtures effects the ligand exchange to produce $[V^{V}O(salen)][Cu_2Cl_4]$ [31]. An amidate ligand H_2phepca reacts with $[VO(acac)_2]$ to afford $[V^{IV}O(phepca)]$ containing a vanadium-deprotonated amide nitrogen bond [32]. The preparation of $[V^{IV}O(thipca)]$ has been achieved by the reaction of *N*-(2-aminophenyl)pyridine-2-carboxamide and 2-mercaptobenzaldehyde with $[VO(CH_3COO)_2]$ [32].

The sodium cation is complexed by [VO(salen)] when a THF or CH_3CN solution of $NaBPh_4$ is treated with [VO(salen)] which affords $[(VO(salen))_2Na][BPh_4]$ containing Na^+ trapped in a coordination cage provided by six oxygen atoms [33]; all the oxygen atoms of [VO(salen)] are involved in coordination to Na^+, giving a cationic polymeric structure.

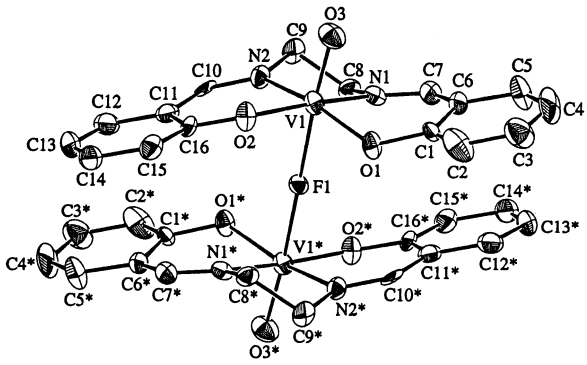

Fig. 3. ORTEP view of $[O=(salen)V-F-V(salen)=O][I_3]\cdot CH_3CN$ (30% probability ellipsoids) [36]: triclinic space group $P\bar{1}$ (#2), $a = 17.10(1)$, $b = 20.38(1)$, $c = 11.813(7)$ Å, $\alpha = 104.08(5)$, $\beta = 98.18(2)$, $\gamma = 75.26(6)^\circ$, $V = 3849(4)$ Å^3, $Z = 4$, $D_{calc} = 1.911$ g cm^{-3}, $\mu(Mo\text{-}K_\alpha) = 29.46$ cm^{-1}, $R = 0.045$, $R_w = 0.075$. Counter anions and hydrogen atoms are omitted for clarity.

3.2. Dinuclear complexes

The $[LV^{IV}-O-LV^{V}=O]^+$ cations such as $[(salen)V^{IV}-O-V^{V}(salen)=O]^+$ [5] have been reported for a number of Schiff base complexes [34]. The $[LV^{IV}-O-LV^{V}=O]^+$ cations have structures that may persist in CH_2Cl_2 where they can undergo redox chemistry, but they apparently dissociate into their component mononuclear complexes in polar solvents such as CH_3CN (Scheme 3) [34].

[VO(salen)] reacted with $HBF_4\cdot Et_2O$ to produce a dinuclear species $[O=(salen)V^{V}-F-V^{V}(salen)=O]^+$, the structure of which was first determined as its BF_4^- and $[VO_2F_2]^-$ salts [35]. The cation was also isolated as triiodide salts as shown in Fig. 3 [36] and Fig. 4 [37].

Reduction of the $[(salen)V^{IV}-O-V^{III}(salen)]^+$ cation by diethylaluminium ethoxide in the presence of phenylhydrazine yields $[V^{III}(PhNHNH_2)_2(salen)][I]$ [38]. The alkylation of $[V^{III}Cl(acen)(THF)]$ using Grignard reagents gives the corresponding organometallic derivatives $[RV(acen)]_2$ ($R = CH_3$, C_6H_5, $C_6H_5CH_2$) having a dimeric structure by sharing one of the oxygen atoms from the Schiff base ligand [39]. The phenolate oxygen in the salen ligand often serves as a bridging ligand; the typical example has been provided by Cu(salen) which crystallizes in a dimeric arrangement with non-planarity of the central coordinated group [40]. A dimeric structure with a V_2O_4 core in the solid state has been found for a dioxovanadium(V) complex with a tridentate asymmetric Schiff base ligand containing primary amine ([1-(*N*-salicylideneamino)-2-aminopropane]dioxovanadium(V)) which can be prepared by the reaction of $VO(OEt)_3$ with salicylaldehyde and the appropriate diamine [41].

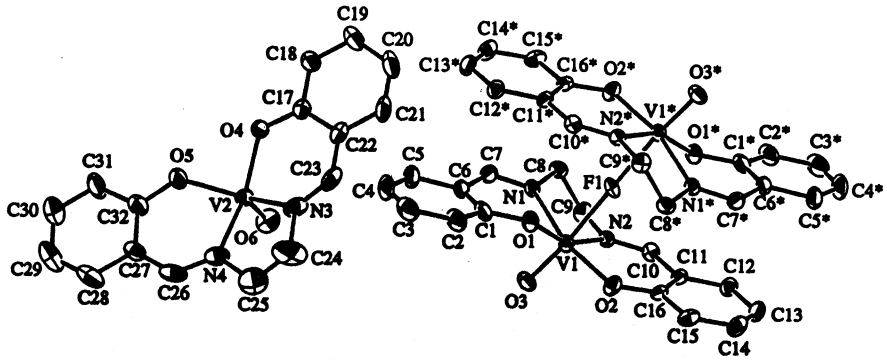

Fig. 4. ORTEP view of [O=(salen)V–F–V(salen)=O][VO(salen)][I_3] (30% probability ellipsoids) [37]: triclinic space group $P\bar{1}$ (#2), $a = 13.983(5)$, $b = 14.764(6)$, $c = 8.729(6)$ Å, $\alpha = 101.65(5)$, $\beta = 99.60(4)$, $\gamma = 108.35(3)^\circ$, $V = 1622(1)$ Å^3, $Z = 1$, $D_{calc} = 1.773$ g cm^{-3}, μ(Mo–K_α) = 20.56 cm^{-1}, $R = 0.061$, $R_w = 0.076$. Counter anions and hydrogen atoms are omitted for clarity.

3.3. Tetranuclear complexes

The 'controlled' protonation of [VO(salen)] with $HBF_4 \cdot Et_2O$ or trityl tetrafluoroborate (in 1:2 mol ratio) yields the tetranuclear complex [(salen)V^{IV}–O–(salen)V^{IV}–O–V^{IV}(salen)–O–V^{IV}(salen)][BF_4]$_2$ containing a linear $V_4^{IV}O_3$ system [42]. The dinuclear complex [(salen)V^{IV}–O–V^{III}(salen)][I_3] dimerizes in crystals, by sharing one of the oxygen atom in the ligand as the bridging atom, to form a tetranuclear complex with the center of symmetry being located at the center of the molecule [42].

3.4. Polynuclear and infinite chains

Atom-bridged linear chain complexes [LM(μ-X)]$_n$ (L = macrocyclic ligands; X=O, F or N) have received much attention for their conductive [43], liquid crystalline [44], and non-linear optical properties [45]. The μ-oxo-bridged linear chain polymers are particularly attractive as electro-optical materials, since linear chain formation could result in unidirectional (head-to-tail) one-dimensional alignment of the M–O dipoles to create non-centrosymmetric assemblies.

Liquid crystals with oxovanadium core groups (metallomesogens) based on the intermolecular interactions in oxovanadium linear chain compounds have been reported for [VO{salptn–(5-RO)$_2$}] (R = C_nH_{2n+1}, $n \geq 4$) [44]. Mesogenic properties of oxovanadium(IV) complexes with rodlike bis(alkylphenylazo)-substituted tetradentate Schiff base ligands *N*,*N*′-bis[5-(4′-*n*-alkyl)phenylazosalicylidene]alkylenediamine based on 1,2-diaminoethane, 1,3-diaminopropane, and 1,3-diamino-2,2-dimethylpropane have also been studied [46].

The crystal structure of [V^{IV}O(salpn)] consists of molecules packed so that the vanadyl oxygen atom of one molecule occupies the sixth position about the vanadium atom in a neighboring molecule [47]. The result is an infinite chain of molecules about a twofold screw axis linked by $\cdots V^{IV}$–O–$V^{IV}\cdots$ bonds. The structure of [V^{IV}O(salptn)] is also polymeric in the solid state with the $\cdots V^{IV}{=}O\cdots V^{IV}{=}O\cdots$ chains, the salptn donor atoms being coplanar and the salptn framework umbrella-shaped [48]. The oxidation of [VO(salen)] with I_2 produces [(salen)V^{IV}–O–V^{V}(salen)=O][I_5]. The cation in the crystal formed a mixed-valent infinite chain ($\cdots V^{IV}{=}O\cdots V^{V}{=}O\cdots$) [49], in contrast to the discrete dinuclear structure found in the triiodide salt [4]. The tetraphenylborate salts of the tetranuclear cations [(salen)V^{IV}–O–(salen)V^{IV}–O–V^{IV}(salen)–O–V^{IV}(salen)] are united to form an infinite chain by sharing one of the phenolate oxygen in the ligand as the bridging atom [42]. Oxovanadium(V) complex with the *p*-methyloxacalix[3]arene ligand is observed to form a μ-oxo bridged linear chain polymer ($\cdots V^{V}{=}O\cdots V^{V}{=}O\cdots$) in the solid state [50].

Interconversion between polymeric and monomeric forms of oxovanadium(IV) complexes with tetradentate Schiff base ligands derived from (*R*,*R*)-2,4-pentanediamine has been reported [51]. The orange crystals of [VO{sal-(*R*,*R*)-2,4-ptn-(3-EtO)$_2$}] have water of crystallization and a polynuclear linear chain structure ($\cdots V^{IV}{=}O\cdots V^{IV}{=}O\cdots$) while the green crystals of the same complex without water of crystallization have a mononuclear square pyramidal structure; dehydration of the orange crystals by heating at 170 °C for 10 min effects the conversion to green crystals which reverts to orange crystals upon re-hydration by suspension in H_2O [51]. On the other hand, only a monomeric structure has been found in [V^{IV}O(sal-(*R*,*R*)-2,4-ptn-(5-MeO)$_2$)] [52].

3.5. Crystal structures and redox-reaction coordinates

Mechanistic interpretations of the energetic aspects of redox reactions often imply a sequence of continuous 'structural changes' along the reaction coordinate. These changes, especially in the region of the transition state, may not be accessible to direct experimental investigation. On the other hand, it should be possible to freeze out the reacting particles into a crystal lattice at any

Table 1
Structural parameters of oxovanadium (III–V) assemblies bearing tetradentate Schiff base ligands derived from α,ω-alkanediamines and salicylaldehyde

Formula	Ligand (L) [a]	Str. [b]	Valence [c]	V–O_{ax} [d] (Å)	V–X_{ax} [e] (Å)	V–N_2O_2 [f] (Å)	V–O_{eq}(av) [g] (Å)	V–N_{eq}(av) [h] (Å)	Reference
$[LV^{IV}=O]$	salen	m	V^{IV} (sp)	1.59		0.609	1.922	2.05	[12]
		m	V^{IV} (sp)	1.587		0.589	1.925	2.056	
	salen	m	V^{IV} (sp)	1.584		0.588	1.920	2.09	[13]
		m	V^{IV} (sp)	1.577		0.595	1.929	2.075	
	salen–(3-*tert*-Bu)$_2$	m	V^{IV} (sp)	1.596		0.6367	1.923	2.057	[29]
	salen–(3-*tert*-Bu)$_2$–(5-Me)$_2$	m	V^{IV} (sp)	1.5913		0.626	1.929	2.065	[15]
	acen	m	V^{IV} (sp)	1.585		0.58	1.95	2.053	[27]
	salpn	p	V^{IV} (oh)	1.633	2.213 (O^*_{ax})	0.31	1.945	2.112	[47]
	salpn–(3-*tert*-Bu)$_2$–(5-Me)$_2$	m	V^{IV} (sp)	1.581		0.531	1.946	2.098	[15]
	salptn	p	V^{IV} (oh)	1.627	2.245 (O^*_{ax})	0.299	1.946	2.094	[48]
	salptn–(3-MeO)$_2$	m	V^{IV} (sp)	1.583		0.53	1.951	2.08	[34]
	sal-(*R*,*R*)-2,4-ptn–(3-EtO)$_2$	m	V^{IV} (sp)	1.582		0.560	1.939	2.086	[51]
$[LV^{IV}=O]\cdot H_2O$	sal-(*R*,*R*)-2,4-ptn–(3-EtO)$_2$	p	V^{IV} (oh)	1.617	2.290 (O^*_{ax})	0.32	1.955	2.106	[51]
	salen–(3-EtO)$_2$	m	V^{IV} (sp)	1.59		0.61	1.93	2.06	[14]
	sal-*meso*-stien–(3-EtO)$_2$	m	V^{IV} (sp)	1.597		0.585	1.930	2.069	[29]
$[LV^{IV}=O]\cdot CH_3OH$	sal-(*R*,*R*)-2,4-ptn–(5-MeO)$_2$	m	V^{IV} (sp)	1.599		0.59	1.945	2.086	[52]
$[LV^{IV}=O(H_2O)]\cdot 0.5H_2O\cdot 0.5CH_3CN$	salton–(3-EtO)$_2$	m	V^{IV} (oh)	1.584	2.406 (QH_2)	0.339	1.955	2.058	[29]
$[LV^{IV}=O(DMSO)]$	salpn	m	V^{IV} (oh)	1.605	2.230 (DMSQ)	0.27	1.962	2.106	[41]
$[LV^{IV}=O(py)]$	sal-(*R*)-pn	m	V^{IV} (oh)	1.589	2.636 (N in py)	0.370	1.947	2.063	[19]
$[(LV^{IV}=O)_2Na][BPh_4]$	salen	d	V^{IV} (sp)	1.584		0.606	1.925	2.045	[33]
$[LV^{V}=O(ClO_4)]$	salen	m	V^{V} (oh)	1.576	2.456 ($QClO_3$)	0.318	1.804	2.079	[17]
$[LV^{V}=O(H_2O)][Cu_2Cl_4]$	salen	m	V^{V} (oh)	1.59	2.31 (QH_2)	0.27	1.819	2.078	[31]
$[LV^{IV}–O–LV^{V}=O][I_3]$	salen	d	V^{V} (oh)	1.573	2.214 (μ-O)	0.270	1.821	2.076	[4]
			V^{IV} (sp)	1.622 (μ-O)		0.55	1.896	2.031	
		d	V^{V} (oh)	1.578	2.246 (μ-O)	0.262	1.834	2.091	
			V^{IV} (sp)	1.612 (μ-O)		0.536	1.916	2.055	
$[LV^{IV}–O–LV^{V}=O]$-$[I_5]\cdot CH_3CN$	salen	p	V^{V} (oh)	1.58	2.06 (μ-O)	0.159	1.795	2.12	[49]
			V^{IV} (oh)	1.67 (μ-O)	2.41 (O^*_{ax})	0.394	1.925	2.025	
$[LV^{IV}–O–LV^{V}=O][ClO_4]$	salen	d	V^{V} (oh)	1.597	2.25 (μ-O)	0.274	1.816	2.086	[5]
			V^{IV} (sp)	1.618 (μ-O)		0.553	1.905	2.049	
$[LV^{IV}–O–LV^{V}=O][ClO_4]$	salen–(5-Me)$_2$	d	V^{V} (oh)	1.58	2.23 (μ-O)	0.272	1.824	2.071	[34]
			V^{IV} (sp)	1.598 (μ-O)		0.542	1.899	2.047	
$[LV^{IV}–O–LV^{V}=O][I_3]$	salen–(5-Me)$_2$	p	V^{V} (oh)	1.588	2.127 (μ-O)	0.241	1.817	2.09	[34]
			V^{IV} (oh)	1.608 (μ-O)	2.36 (O^*_{ax})	0.383	1.901	2.03	
$[LV^{IV}–O–LV^{V}=O][I_3]$	sal-1,2-pn	d	V^{V} (oh)	1.59	2.18 (μ-O)	0.251	1.79	2.075	[34]
			V^{IV} (sp)	1.63 (μ-O)		0.541	1.895	1.945	

Table 1 (*Continued*)

Formula	Ligand (L) [a]	Str. [b]	Valence [c]	V–O_{ax} [d] (Å)	V–X_{ax} [e] (Å)	V–N_2O_2 [f] (Å)	V–O_{eq}(av) [g] (Å)	V–N_{eq}(av) [h] (Å)	Reference
$[O{=}LV^{V}_{\alpha}{-}F{-}LV^{V}_{\beta}{=}O][BF_4]$	salen	d	V^{V}_{α} (oh)	1.59	2.087 (μ-F)	0.228	1.831	2.077	[35]
			V^{V}_{β} (oh)	1.59	2.036 (μ-F)	0.206	1.82	2.078	
		d	V^{V}_{α} (oh)	1.60	2.039 (μ-F)	0.217	1.824	2.094	
			V^{V}_{β} (oh)	1.59	2.064 (μ-F)	0.234	1.8345	2.077	
$[O{=}LV^{V}_{\alpha}{-}F{-}LV^{V}_{\beta}{-}O][I_3]\cdot CH_3CN$	salen	d	V^{V}_{α} (oh)	1.589	2.094 (μ-F)	0.243	1.825	2.078	[36]
			V^{V}_{β} (oh)	1.585	2.074 (μ-F)	0.225	1.826	2.077	
		d	V^{V}_{α} (oh)	1.590	2.058 (μ-F)	0.209	1.827	2.087	
			V^{V}_{β} (oh)	1.583	2.073 (μ-F)	0.212	1.826	2.091	
$[O{=}LV^{V}{-}F{-}LV^{V}{=}O]{-}[LV^{IV}{=}O][I_3]$	salen	d	V^{V} (oh)	1.601	2.06 (μ-F)	0.207	1.833	2.092	[37]
		m	V^{IV} (sp)	1.595		0.587	1.933	2.054	
$[LV^{IV}{-}O{-}LV^{III}][I_3]$	salen	t	V^{IV} (sp)	1.646 (μ-O)		0.534	1.906	2.050	[5,42]
			V^{III} (oh)	2.014 (μ-O)	2.101 (O^{*}_{eq})	0.059	1.916	2.083	
$[LV^{IV}_{\alpha}{-}O_{\alpha}{-}LV^{IV}_{\beta}{-}O_{\beta}{-}LV^{IV}{-}O{-}LV^{IV}]$ $[BF_4]_2\cdot 2CH_3CN$	salen	t	V^{IV}_{α} (sp)	1.625 (O_{α})		0.541	1.896	2.036	[42]
			V^{IV}_{β} (oh)	1.763 (O_{β})	2.059 (O_{α})	0.141	1.830	2.079	
$[LV^{IV}_{\alpha}{-}O_{\alpha}{-}LV^{IV}_{\beta}{-}O_{\beta}{-}LV^{IV}{-}O{-}LV^{IV}]$ $[BPh_4]_2\cdot 2CH_3CN$	salen	p	V^{IV}_{α} (oh)	1.627 (O_{α})	2.289 (O^{*}_{eq})	0.303	1.96	2.060	[42]
			V^{IV}_{β} (oh)	1.775 (O_{β})	2.095 (O_{α})	0.151	1.835	2.072	

[a] For ligand structures, see Appendix A.

[b] Packing structures in crystals: m, mononuclear; d, dinuclear; t, tetranuclear; p, polynuclear (infinite chain).

[c] Oxidation states of vanadium atoms. Coodination geometry in parenthesis: sp, square pyramidal; oh, octahedral.

[d] Distance between vanadium atoms and axial oxygen atoms O_{ax} shown in parenthesis. Unless noted, O_{ax} are vanadyl oxygen atoms.

[e] Distance between vanadium atoms and axial donor atoms X shown in parenthesis. The atoms X occupy the position *trans* to the vanadyl oxygen atoms. The atoms generated by symmetry expansion are shown with asterisks.

[f] Displacement of vanadium atoms from the N_2O_2 best least-squares planes of Schiff base ligands.

[g] Mean distance between vanadium atoms and equatorial oxygen atoms in Schiff base ligands.

[h] Mean distance between vanadium atoms and equatorial nitrogen atoms in Schiff base ligands.

point along the redox-reaction coordinate by suitable perturbations such as crystal packing forces. However, it is practically difficult to vary such perturbations in a systematic way to sample a number of points along the reaction coordinate. An alternative approach has been reported [53] trying to derive the detailed structural pathway for a particular type of reaction by searching for certain kinds of correlations in a set of selected structural data obtained from a number of crystal structure analyses.

A similar approach could be made to derive the redox-reaction coordinates to represent the structural changes occurring in the V(IV)/V(III) and V(V)/V(IV) redox reactions. Structural parameters of a variety of oxovanadium complexes bearing tetradentate Schiff base ligands and their assemblies, including those of the crystallographic polymorphs, are compiled in Table 1. The coordination geometry around oxovanadim centers can be represented by three major parameters: the V–O_{ax} bond distance, the deviation of vanadium atoms out of the equatorial plane and the distance to external axial ligands *trans* to the vanadyl oxygen atom. The atomic arrangements around vanadium atoms can be regarded as square pyramids or octahedra with N_2O_2 equatorial atoms and various axial ligands. Fig. 5 shows the observed structural parameters for 52 different arrangement of ligands about vanadium atoms, which reveals a correlation between the V–O_{ax} bond length and the non-planarity of the V–N_2O_2 fragment. The main trend observed for six-coordinate vanadium centers are as follows: the oxidation of vanadium(III) typically in an octahedral arrangement to vanadium(IV), and finally to vanadium(V), is accompanied by the significant shortening of the V–O_{ax} bond length and by the extensive deviation of vanadium atoms out of the N_2O_2 plane whereas the V–N_{eq} length remains constant. These atomic arrangements could represent a sequence of frozen-in points along the reaction coordinate of the redox reactions of V(IV)/V(III) and V(V)/V(IV).

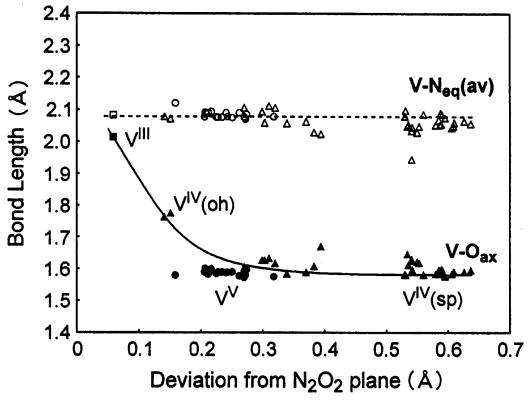

Fig. 5. Relationship between selected structural parameters of oxovanadium mononuclear complexes and their linear assemblies with tetradentate Schiff base ligands from Table 1.

The redox-reaction coordinate (Fig. 5) not only yields details of the sequence of structural changes that occur in the course of multielectron redox reactions, but also provides estimates for the origin of driving forces that promotes the splitting of O_2. As to the reaction of the $[LV^{IV}–O–LV^{III}]^+$ cation with O_2 to $[LV^{IV}–O–LV^{V}=O]^+$ (Scheme 4), it is obvious from Fig. 5 that the six-coordinate distorted octahedral arrangement around vanadium(IV), which is perturbed from the square pyramidal five-coordination typically observed for vanadium(IV) and is rather close to the preferred geometry around vanadium(V), would afford the driving force for the homolytic cleavage of the μ-dioxo bond in the $[LV^{IV}–O–LV^{IV}–O–O–LV^{IV}–O–LV^{IV}]^{2+}$ cation (Scheme 5). It also provides an account for the disproportionation of six-coordinate vanadium(IV) complexes to vanadium(III) and vanadium(V) (vide infra) [6].

4. Coordination chemistry and multielectron redox reactions

The acid–base, coordination and redox chemistries of vanadium complexes in oxidation states III–V with tetradentate Schiff base ligands have been widely studied [17]. In anhydrous CH_3CN, addition of stoichiometric quantities of CF_3SO_3H to solutions of $[V^{IV}O(salen)]$ produces $[V^{V}O(salen)]^+$, $[V^{III}(salen)]^+$ and H_2O [18]. In contrast, a μ-oxo divanadium(IV) complex $[(salen)V^{IV}–O–V^{IV}(salen)]^{2+}$ is produced in CH_2Cl_2 which is converted to $[V^{IV}(salen)]^{2+}$ in the presence of significant excesses of CF_3SO_3H [6]. In CH_2Cl_2 solutions containing a large amount of an electrolyte such as tetrabutylammonium tetrafluoroborate, the $[(salen)V^{IV}–O–V^{IV}(salen)]^{2+}$ complex undergoes disproportionation and dissociation reactions to produce a solution containing an equimolar mixture of $[V^{IV}O(salen)]$, $[V^{III}(salen)]^+$, and $[(salen)V^{IV}–O–V^{V}(salen)]^{3+}$. Physical parameters for these reactions such as equilibrium constants and formal potentials have been determined.

4.1. Disproportionation in polar solvents

The solution of $[LV^{IV}=O]$ with CF_3SO_3H in anhydrous CH_3CN provokes an acid-induced disproportionation of $[LV^{IV}=O]$ according to $2[LV^{IV}=O]+2H^+ \rightleftarrows [LV^{V}=O]^+ + [LV^{III}]^+ + H_2O$ [18]. The equilibrium constants for the disproportionation have been determined (Table 2). The two-electron reduction of $[LV^{V}=O]^+$ to $[LV^{III}]^+$ via disproportionation of $[LV^{IV}=O]$, according to the stoichiometry $[LV^{V}=O]^+ + 2H^+ + 2e^- \rightarrow [LV^{III}]^+ + H_2O$, has been established [54]. The disproportionation of $[LV^{IV}=O]$ goes to completion in the absence of BF_4^- [55] (more basic than CF_3SO_3H [18]) or excess H_2O [56] but reaches an intermediate equilibrium

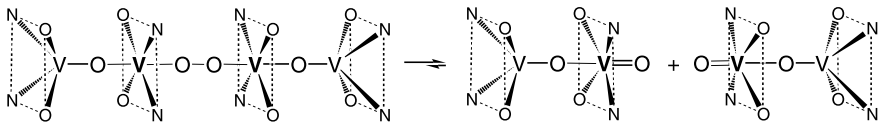

Scheme 5.

state in their presence unless significant excesses of acid are added. The formal potentials for the redox couples related to the disproportionation of $[LV^{IV}{=}O]$ have also been determined (Table 2). The formal potentials in Table 2 show that in the presence of acid, $[LV^{IV}{=}O]$ is a considerably stronger one-electron oxidant than is $[LV^{V}{=}O]^{+}$, which accounts for the acid-induced disproportionation of $[LV^{IV}{=}O]$. The equilibrium constant of 42 M^{-1} has been calculated for $[V^{IV}O(salen)]+2H^{+} \leftrightarrows [V^{IV}(salen)]^{2+}+H_2O$ in CH_3CN [18]. The acid-induced disproportionation reaction in CH_3CN has been considered to begin with the removal of the oxo ligand from $[LV^{IV}{=}O]$ by the added acid followed by an outer-sphere oxidation of a second $[LV^{IV}{=}O]$ molecule by $[LV^{IV}]^{2+}$ according to $[LV^{IV}{=}O]+[LV^{IV}]^{2+} \leftrightarrows [LV^{V}{=}O]^{+}+[LV^{III}]^{+}$ [18]. An equilibrium constant of $[V^{V}O(salen)^{+}][V^{III}(salen)^{+}][V^{IV}O(salen)]^{-1}[V^{IV}(salen)^{2+}]^{-1} = 3.8\times10^{4}$ has been calculated (Table 2) [18].

4.2. Dimerization and disproportionation in non-polar solvents

The μ-oxo divanadium(IV) cation $[(salen)V^{IV}{-}O{-}V^{IV}(salen)]^{2+}$ can be prepared by the acidification of [VO(salen)] with CF_3SO_3H or trityl tetrafluoroborate in non-aqueous media ($2[V^{IV}O(salen)]+2H^{+} \rightarrow [(salen)V^{IV}{-}O{-}V^{IV}(salen)]^{2+}+H_2O$) [55]. In CH_2Cl_2, the conversion of $[V^{IV}O(salen)]$ to $[(salen)V^{IV}{-}O{-}V^{IV}(salen)]^{2+}$ is extensive; the dinuclear complex has been isolated as the tetrafluoroborate salt [55]. Attempts to obtain single crystals of $[(salen)V^{IV}{-}O{-}V^{IV}(salen)][BF_4]_2$ have met with failure which can be reasoned by the spontaneous disproportionation of the μ-oxo divanadium(IV) complex (vide infra). On the other hand, the reduction of the μ-oxo divanadium(IV) complex by tetrabutylammonium iodide produces a mixed-valent μ-oxo divanadium(III, IV) complex $[(salen)V^{IV}{-}O{-}V^{III}(salen)][I_3]$ which has been isolated as single crystals (Fig. 1(a)) [5]. The μ-oxo divanadium(III, IV) complex can also be obtained by the electrochemical reduction of the divanadium(IV) complex under argon at potentials lower than +0.1 V versus Fc/Fc^{+} couple which consumed one electron per mole of complex as expected for the quantitative reduction ($[(salen)V^{IV}{-}O{-}V^{IV}(salen)]^{2+}+e^{-} \rightarrow [(salen)V^{IV}{-}O{-}V^{III}(salen)]^{+}$) [4]. Addition of HI to solutions of [VO(salen)] in acetonitrile also gives $[(salen)V{-}O{-}V(salen)][I_3]$ [42]. It can be reasoned that acidification of [VO(salen)] with HI would first result in dimerization of [VO(salen)] and then in subsequent reduction by iodide to produce $[(salen)V{-}O{-}V(salen)][I_3]$ [5]. The mixed-valent state has been characterized by the near-infrared spectrum [5]. An intervalence transition band has been observed at $\nu_{max} = 7.2\times10^{3}$ cm^{-1} in acetonitrile with half band width $\Delta_{1/2}$ of 3.0×10^{3} cm^{-1} and molar absorption coefficient ε_{max} of 60.1 M^{-1} cm^{-1} which has been

Table 2
Equilibrium constants (K) and formal potentials (E^{f}) of vanadium complexes with tetradentate Schiff base ligands related to acid-induced disproportionation of oxovanadium(IV) ($2[LV^{IV}{=}O]+2H^{+} \leftrightarrows [LV^{V}{=}O]^{+}+[LV^{III}]^{+}+H_2O$) in CH_3CN

Complex ($[LV^{IV}{=}O]$) [a]	K [b] (M^{-1})	$E^{f}(1)$ [c] (V vs. Fc/Fc^{+})	$E^{f}(2)$ [d] (V vs. Fc/Fc^{+})	$E^{f}(3)$ [e] (V vs. Fc/Fc^{+})	$E^{f}(4)$ [f] (V vs. Fc/Fc^{+})	Reference
$[V^{IV}O(salen)]$	$(1.6\pm0.3)\times10^{6}$	0.07	0.34	0.26	0.44	[18]
$[V^{IV}O(salen{-}(3,5\text{-di-}\textit{tert}\text{-Bu})_2)]$	$(6\pm4)\times10^{7}$	−0.04	0.16	0.19	0.41	[54]
$[V^{IV}O(salphen)]$	$(3.3\pm0.3)\times10^{5}$	0.20	0.51	0.37	0.53	[54]
$[V^{IV}O(salphen{-}(3,5\text{-di-}\textit{tert}\text{-Bu})_2)]$	$(1.0\pm0.3)\times10^{6}$	0.16	0.28	0.34	0.51	[54]
$[V^{IV}O(salen{-}(5\text{-MeO})_2)]$	$(3\pm2)\times10^{7}$	0.01	0.18	0.23	0.44	[54]
$[V^{IV}O(salen{-}(4,6\text{-di-MeO})_2)]$	$(5\pm3)\times10^{7}$	−0.01	0.26	0.22	0.44	[54]
$[V^{IV}O(nalphen)]$	$(3.0\pm0.5)\times10^{5}$	0.21	0.46	0.37	0.53	[54]

[a] For ligand structures, see Appendix A.
[b] $K = [LV^{V}{=}O^{+}][LV^{III+}][H_2O][LV^{IV}{=}O]^{-2}[H^{+}]^{-2}$ at 22 °C.
[c] For half reaction (1): $[LV^{V}{=}O]^{+}+e^{-} = [LV^{IV}{=}O]$.
[d] For half reaction (2): $[LV^{IV}]^{2+}+e^{-} = [LV^{III}]^{+}$.
[e] For half reaction (3): $[LV^{V}{=}O]^{+}+2H^{+}+2e^{-} = [LV^{III}]^{+}+H_2O$.
[f] For half reaction (4): $[LV^{IV}{=}O]+2H^{+}+e^{-} = [LV^{III}]^{+}+H_2O$.

determined by considering the dissociation equilibrium of the complex in acetonitrile ([VO(salen)][V(salen)$^+$]/[(salen)VOV(salen)$^+$] = 13 mM) [5]. The crystal structure provides the non-bonding vanadium(III)-to-vanadium(IV) distance of $r = 3.569$ Å in the dinuclear complex. The interaction factor α of the mixed-valent state has been determined to be 3.0×10^{-2} where $\alpha^2 = (4.5 \times 10^{-4})\varepsilon_{max}\Delta_{1/2}\nu^{-1}r^{-2}$. (The extent of interaction is defined for the ground state of the complex as $\Psi_G = (1-\alpha^2)^{1/2}\Phi_i + \alpha\Phi_j$ where Φ_i and Φ_j are wave functions for the donor–acceptor components of the mixed valence systems [57].) The complex has thus been classified into a Type II mixed-valent complex.

The μ-oxo divanadium(IV, V) complex [(salen)V^{IV}–O–V^{V}(salen)]$^{3+}$ can be prepared by the reaction of the [(salen)V^{IV}–O–V^{V}(salen)=O]$^+$ cation with a strong acid such as CF_3SO_3H to undergo deoxygenation of the terminal oxo group ([(salen)V^{IV}–O–V^{V}(salen)=O]$^+ + 2H^+ \rightarrow$ [(salen)V^{IV}–O–V^{V}(salen)]$^{3+} + H_2O$) [5]. The coulometric one-electron oxidation of [(salen)V^{IV}–O–V^{IV}(salen)]$^{2+}$ at potentials higher than +0.1 V versus Fc/Fc$^+$ also gives [(salen)V^{IV}–O–V^{V}(salen)]$^{3+}$ [5]. While the [(salen)V^{IV}–O–V^{V}(salen)=O]$^+$ cation shows no absorption in the near-infrared spectrum, the solution of [(salen)V^{IV}–O–V^{V}(salen)]$^{3+}$ exhibited a weak intervalence transition band with $\nu_{max} = 7.1 \times 10^3$ cm^{-1}, $\Delta_{1/2}$ of 3.2×10^3 cm^{-1} and ε_{max} of 10 M^{-1} cm^{-1} at the ν_{max} [5].

Steady-state voltammograms at rotating disk electrodes in solutions prepared by dissolving [(salen)V^{IV}–O–V^{IV}(salen)][BF_4]$_2$ in CH_2Cl_2 containing tetrabutylammonium tetrafluoroborate exhibit a single composite wave consisting of equal anodic and cathodic plateau currents at $E_{1/2} = 0.10$ V versus Fc/Fc$^+$ [58]. Electrolysis of solutions of [(salen)V^{IV}–O–V^{IV}(salen)][BF_4]$_2$ at 0 or 0.2 V versus Fc/Fc$^+$ showed that both the oxidation and the reduction processes involve one electron per molecule of [(salen)V^{IV}–O–V^{IV}(salen)][BF_4]$_2$ dissolved in the initial solution. The presence of a single composite voltammetric wave instead of separated oxidation and reduction waves at different potentials suggest that the formal potential of the [(salen)V–O–V(salen)]$^{3+/2+}$ couple is less positive than that of the [(salen)V–O–V(salen)]$^{2+/+}$ couple so that spontaneous disproportionation of [(salen)V^{IV}–O–V^{IV}(salen)]$^{2+}$ into [(salen)V^{IV}–O–V^{V}(salen)]$^{3+}$ and [(salen)V^{IV}–O–V^{III}(salen)]$^+$ can occur [6]. Solutions of [(salen)V^{IV}–O–V^{IV}(salen)]$^{2+}$ in pure CH_2Cl_2 exhibit no ESR signal but addition of tetrabutylammonium tetrafluoroborate produces a spectrum indicating the presence of [V^{V}O(salen)]. This behavior is consistent with the disproportionation of [(salen)V^{IV}–O–V^{IV}(salen)]$^{2+}$ to produce two ESR-silent products according to 2[(salen)V^{IV}–O–V^{IV}(salen)]$^{2+} \rightarrow$ [(salen)V^{IV}–O–V^{III}(salen)]$^+$ + [(salen)V^{IV}–O–V^{V}(salen)]$^{3+}$ followed by the spontaneous dissociation of the [(salen)V^{IV}–O–V^{III}(salen)]$^+$ complex to produce the ESR-active [V^{IV}O(salen)] complex and the ESR-silent [V^{III}(salen)]$^+$ complex according to [(salen)V^{IV}–O–V^{III}(salen)]$^+ \rightarrow$ [V^{IV}O(salen)] + [V^{III}(salen)]$^+$. The sum of the reactions, 2[(salen)V^{IV}–O–V^{IV}(salen)]$^{2+} \rightarrow$ [(salen)V^{IV}–O–V^{V}(salen)]$^{3+}$ + [V^{IV}O(salen)] + [V^{III}(salen)]$^+$, proceeds essentially to completion in the presence of 0.1 M tetrabutylammonium tetrafluoroborate to produce one reducible and two oxidizable complexes [6]. The equal anodic and cathodic plateau currents obtained for the solution prepared by dissolving [(salen)V^{IV}–O–V^{IV}(salen)]$^{2+}$ in CH_2Cl_2 in the presence of tetrabutylammonium tetrafluoroborate [58] can be ascribed to the simultaneous one-electron oxidation of [V^{III}(salen)]$^+$ and [V^{IV}O(salen)] and the two-electron reduction of [(salen)V^{IV}–O–V^{V}(salen)]$^{3+}$, respectively [6]. The effect of the electrolyte may be to facilitate the encounter of the two cations involved in the disproportionation of [(salen)V^{IV}–O–V^{IV}(salen)]$^{2+}$ or to enhance the dissociation of [(salen)V^{IV}–O–V^{III}(salen)]$^+$ by stabilization of the coordinatively unsaturated [V^{III}(salen)]$^+$ complex [6].

If significant excesses of acid are added to the solutions of [(salen)V^{IV}–O–V^{IV}(salen)]$^{2+}$, the dimeric cation undergoes further reaction to produce 2 mol of the [V^{IV}(salen)]$^{2+}$ complex [6]. The acid cleavage of [(salen)V^{IV}–O–V^{IV}(salen)]$^{2+}$ has been followed with ESR spectroscopy. Addition of stoichiometric quantities (or small stoichiometric excesses) of CF_3SO_3H to a solution of [V^{IV}O(salen)] caused the initial ESR signal to diminish greatly because of magnetic coupling through the oxo bridge in the dimeric [(salen)V^{IV}–O–V^{IV}(salen)]$^{2+}$ complex [55]. Addition of excess CF_3SO_3H caused a new spectrum to appear that is attributed to [V^{IV}(salen)]$^{2+}$ produced according to [(salen)V^{IV}–O–V^{IV}(salen)]$^{2+} + 2H^+ \rightleftarrows$ 2[V^{IV}(salen)]$^{2+} + H_2O$ [6]. The g_0 value for the [V^{IV}(salen)]$^{2+}$ complex (1.960) is smaller than that of typical oxovanadium(IV) complexes ($g_0 = 1.97$–1.99 [59]) which is a feature commonly observed for four-coordinate vanadium(IV) complexes [60] and indicates that under sufficiently acidic conditions, the oxo groups in both [V^{IV}O(salen)] and [(salen)V^{IV}–O–V^{IV}(salen)]$^{2+}$ are removed. Stoichiometric quantities of protons are adequate for essentially complete conversion of [V^{IV}O(salen)] into [(salen)V^{IV}–O–V^{IV}(salen)]$^{2+}$ while the conversion of [(salen)V^{IV}–O–V^{IV}(salen)]$^{2+}$ into [V^{IV}(salen)]$^{2+}$ requires a considerable excess of protons. An equilibrium constant of [V^{IV}(salen)$^{2+}$]^2[H_2O]-[(salen)V^{IV}–O–V^{IV}(salen)$^{2+}$]$^{-1}$[H^+]$^{-2} \sim 6 \times 10^{-4}$ has been obtained [6]. The relatively small value of this constant reflects the stability of [(salen)V^{IV}–O–V^{IV}(salen)]$^{2+}$ toward acid cleavage. The formal potential of 0.09 V versus Fc/Fc$^+$ has been obtained for the [V(salen)]$^{2+/+}$ couple which is essentially the same as

the formal potential of the $[VO(salen)]^{+/0}$ couple in CH_2Cl_2.

5. Catalytic reactions related to O_2

Oxovanadium(IV) complexes have been used as catalysts in the epoxidation of olefins and in the oxidation of sulfides with peroxides [61]. Among the useful features of oxovanadium complexes is their ability to serve as catalysts for the oxidative polymerization of diphenyl disulfide using O_2 as an oxidant and the electroreduction of O_2 to H_2O under acidic conditions. Because the electroreduction of O_2 by four electrons usually requires catalysts such as dimeric [62] or multinuclear [63] metalloporphyrin complexes that are difficult to synthesize, the easily prepared vanadium Schiff base complexes are attractive as alternative catalysts. Possible mechanisms for both the stoichiometric four-electron electroreduction of O_2 in acid-free solutions and the catalytic four-electron reduction in the presence of excess acid have been proposed.

5.1. Electroreduction of O_2

Cyclic voltammograms for solutions of $[V^{IV}O(salen)]$ with tetrabutylammonium tetrafluoroborate as a supporting electrolyte exhibit a reversible response for $[VO(salen)]^{+/0}$ couple at 0.08 and 0.09 V versus Fc/Fc^+ in CH_3CN [18] and CH_2Cl_2 [6], respectively. This response is unaffected by the presence of O_2, which does not react with $[V^{IV}O(salen)]$ or $[V^{V}O(salen)]^+$ at a significant rate in the absence of acid. Acid-free solutions of $[V^{IV}O(salen)]$ exhibit no cathodic electrochemistry at potentials positive of -1.9 V versus Fc/Fc^+.

The $[LV^{III}]^+$ complexes such as $[V^{III}(salen)]^+$ in CH_3CN react with O_2 to produce $[LV^{V}{=}O]^+$ according to $2[LV^{III}]^+ + O_2 \rightarrow 2[LV^{V}{=}O]^+$ [18]. The kinetics of the reaction have been examined by monitoring the increase in the concentration of $[LV^{V}{=}O]^+$ [54]. The reaction rate is first-order with respect to $[LV^{III}]^+$ and O_2, respectively. A mechanism consistent with this behavior is given in Scheme 6 [54]. Applying the steady-state approximation to $[LV{-}O_2]^+$ and $[LV{-}O{-}O{-}LV]^{2+}$ leads to the rate law $-d[LV^{III+}]/dt = 2k_1k_2[LV^{III+}]^2[O_2]/(k_{-1}+k_2[LV^{III+}])$. The observed first order dependence of the rate on $[LV^{III}]^+$ implies

$$[LV^{III}]^+ + \mathbf{O_2} \underset{k_{-1}}{\overset{k_1}{\rightleftharpoons}} [LV\text{-}\mathbf{O_2}]^+$$

$$[LV\text{-}\mathbf{O_2}]^+ + [LV^{III}]^+ \xrightarrow{k_2} [LV\text{-}\mathbf{O}\text{-}\mathbf{O}\text{-}LV]^{2+}$$

$$[LV\text{-}\mathbf{O}\text{-}\mathbf{O}\text{-}LV]^{2+} \xrightarrow[\text{(fast)}]{k_3} 2\,[LV^{V}{=}\mathbf{O}]^+$$

Scheme 6.

Table 3
Rate constants for the oxidation of $[LV^{III}]^+$ by O_2 [a]

Complex ($[LV^{III}]^+$) [b]	k_1 [c] ($M^{-1}\,s^{-1}$)	Reference
$[V^{III}(salen)]^+$	0.07	[18]
	0.060 ± 0.003	[54]
$[V^{III}(salen{-}(3,5\text{-di-}tert\text{-}Bu)_2)]^+$	0.44 ± 0.02	[54]
$[V^{III}(salphen)]^+$	0.060 ± 0.003	[54]
$[V^{III}(salphen{-}(3,5\text{-di-}tert\text{-}Bu)_2)]^+$	0.46 ± 0.02	[54]
$[V^{III}(salen{-}(5\text{-}MeO)_2)]^+$	0.13 ± 0.01	[54]
$[V^{III}(salen{-}(4,6\text{-di-}MeO)_2)]^+$	0.11 ± 0.01	[54]
$[V^{III}(nalphen)]^+$	0.090 ± 0.005	[54]

[a] $2[LV^{III}]^+ + O_2 \rightarrow 2[LV^{V}{=}O]^+$.
[b] For ligand structures, see Appendix A.
[c] $-d[LV^{III+}]/dt = 2k_1[LV^{III+}][O_2]$.

that $k_{-1} < k_2[LV^{III+}]$; the rate law in this case becomes $-d[LV^{III+}]/dt = 2k_1[LV^{III+}][O_2]$ [18]. Table 3 provides the values of k_1 determined for seven complexes of $[LV^{III}]^+$ at 22 °C [18]. The reaction can occur both in the absence and in the presence of acid, but the reduction of O_2 stops when all of the $[LV^{III}]^+$ is oxidized to $[LV^{V}{=}O]^+$. However, in the presence of excess acid, the regeneration of $[LV^{III}]^+$ (via $[LV^{V}{=}O]^+ + 2H^+ + 2e^- \rightarrow [LV^{III}]^+ + H_2O$) provides a route for the four-electron electroreduction of O_2 as catalyzed by $[LV^{IV}{=}O]$. For $[VO(salen)]$ in CH_3CN, the rate of the catalytic cycle is too slow because CH_3CN molecules coordinated to the axial sites in $[V^{III}(salen)]^+$ could retard the coordination of O_2 to $[V^{III}(salen)]^+$, and in addition, the acid-induced decomposition of $[V^{III}(salen)]^+$ is rapid [18]. On the other hand, $[V^{IV}O(salphen{-}(3,5\text{-di-}tert\text{-}Bu)_2)]$ can act as a catalyst for the electroreduction of O_2 to H_2O without significant decomposition of the catalyst [54]. When a porous glassy-carbon electrode is introduced into the solution to carry out the electroreduction of $[V^{V}O(salphen{-}(3,5\text{-di-}tert\text{-}Bu)_2)]^+$ to $[V^{III}(salphen{-}(3,5\text{-di-}tert\text{-}Bu)_2)]^+$ via $[V^{IV}O(salphen{-}(3,5\text{-di-}tert\text{-}Bu)_2)]$, the cathodic charge consumed with O_2-saturated CH_3CN is much greater than that consumed with argon-saturated solutions, and corresponds to the amount of the acid [54]. More than 60 turn-overs of the catalyst occurred without significant decomposition of the catalyst.

In acidified CH_2Cl_2 in the absence of O_2, the electroreduction of $[V^{IV}O(salen)]$ also proceeds accord-

$$[LV^{IV}{=}O] + 2H^+ \rightleftharpoons [LV^{IV}]^{2+} + H_2O$$

$$[LV^{IV}{=}O] + [LV^{IV}]^{2+} \rightarrow [LV^{IV}\text{-}O\text{-}LV^{IV}]^{2+}$$

$$2\,[LV^{IV}\text{-}O\text{-}LV^{IV}]^{2+} \rightarrow [LV^{IV}\text{-}O\text{-}LV^{III}]^+ + [LV^{IV}\text{-}O\text{-}LV^{V}]^{3+}$$

$$[LV^{IV}\text{-}O\text{-}LV^{V}]^{3+} + 2e^- \rightarrow [LV^{IV}\text{-}O\text{-}LV^{III}]^+$$

$$[LV^{IV}\text{-}O\text{-}LV^{III}]^+ \rightarrow \mathbf{[LV^{III}]^+} + [LV^{IV}{=}O]$$

Scheme 7.

ing to $[V^{IV}O(salen)]+2H^{+}+e^{-}\rightarrow[V^{III}(salen)]^{+}+H_2O$ but the mechanism that produces this stoichiometry involves the acid cleavage, disproportionation, and inner-sphere redox reactions as shown in Scheme 7. The catalytic reduction by $[V^{III}(salen)]^{+}$ proceeds readily in CH_2Cl_2. Electrolysis of acidified $[V^{IV}O(salen)]$ solutions that are saturated with O_2 results in the consumption of many electrons per $[V^{IV}O(salen)]$ complex [6]. The reduced, deoxygenated $[V^{III}(salen)]^{+}$ complex is the essential species in the catalysis of the electroreduction of O_2 by four electrons in CH_2Cl_2. The binuclear complexes $[(salen)V^{IV}–O–V^{IV}(salen)]^{2+}$ and $[(salen)V^{IV}–O–V^{V}(salen)]^{3+}$ is the reservoir from which the active $[V^{III}(salen)]^{+}$ complex is generated by disproportionation of $[(salen)V^{IV}–O–V^{IV}(salen)]^{2+}$ followed by dissociation of $[(salen)V^{IV}–O–V^{III}(salen)]^{+}$ [6]. The four-electron reduction of O_2 to two coordinated oxo ligands and ultimately to two H_2O molecules is accomplished by the cycling of the V(salen) group between its $[V^{III}(salen)]^{+}$ and $[V^{V}O(salen)]^{+}$ oxidation states. The breaking of the O–O bond in O_2 is fostered by the oxophilic character of the vanadium(V) state of the catalyst. The activity of the $[V^{III}(salen)]^{+}$ complex is higher when the CH_2Cl_2 solvent is treated with $(CF_3CO)_2O$ because the coordination of H_2O and especially OH^{-} to the vanadium(III) center interferes with the binding of O_2 to the same coordination site that is required in the inner-sphere, catalytic electron-transfer mechanism [6].

In other studies, the formation of a $[V(salen)–O_2]^{+}$ complex has also been examined in pyridine [64]. However, the reaction of $[V(salen)]^{+}$ with O_2 proceeds only to $[V^{IV}O(salen)]$ in pyridine. Oxidation of bis(maltolato)oxovanadium(IV) ($VO(ma)_2$) by O_2 in CH_3OH produces *cis*-$V^{V}O(OCH_3)(ma)_2$ ($2VO(ma)_2+1/2O_2+2CH_3OH\rightarrow2VO(OCH_3)(ma)_2+H_2O$), which has been proposed to proceed through a μ-dioxo-bridged vanadium(V) complex (Scheme 8) [65].

5.2. O_2-oxidation and oxidative polymerization of aromatic compounds

The catalytic oxidation of pyrrole by the $[(salen)V^{IV}–O–V^{V}(salen)]^{3+}$ cation formed on an electrode surface by the oxidation of $[(salen)V^{IV}–O–V^{IV}(salen)]^{2+}$ has been examined by hydrodynamic voltammetry at a rotating glassy carbon disk electrode [66]. The electron

$$V^{IV}O(ma)_2 + O_2 \longrightarrow VO(ma)_2(O_2)$$

$$VO(ma)_2(O_2) + VO(ma)_2 \longrightarrow VO(ma)_2(\mu\text{-}OO)VO(ma)_2$$

$$VO(ma)_2(\mu\text{-}OO)VO(ma)_2 + 2\,CH_3OH \longrightarrow 2\,VO(OCH_3)(ma)_2 + H_2O_2$$

$$H_2O_2 \longrightarrow 1/2\,O_2 + H_2O$$

Scheme 8.

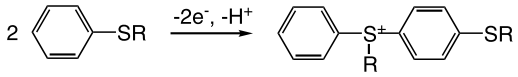

(R = C_nH_{2n+1}, n = 1-3)

Scheme 9.

transfer rate constant for the cross-reaction $[(salen)V^{IV}–O–V^{V}(salen)]^{3+}$/pyrrole has been estimated to be $4\times10^{4}\ mol^{-1}\ cm^{3}\ s^{-1}$. O_2-oxidation of the $[(salen)V^{IV}–O–V^{III}(salen)]^{+}$ cation gives rise to the catalysis for the O_2-oxidative polymerization of pyrrole. With [VO(salen)] as a catalyst, polypyrrole is obtained only in the presence of acid such as CF_3SO_3H. In contrast, the μ-oxo divanadium cation catalyzed the oxidative polymerization of pyrrole in the absence of the acid. The μ-oxo divanaium cation produced from [VO(salen)] under acidic conditions is likely to act as a catalyst. Under an argon atmosphere, only a small amount of polymer is obtained, which suggests that O_2 acts as an oxidant in the polymerization. The polymerization is rate-determined by the reoxidation step of the catalyst by O_2. The turnover number of 60 for the μ-oxo divanaium cation [66] is much higher than the previously reported values of 2.5–6.5 for the conventional catalysts such as $VO(acac)_2$–$AlCl_3$ and $FeCl_3$ [67]

The oxidative coupling of arylsulfides using O_2 as an oxidant can be catalyzed by $VO(acac)_2$ in the presence of tetrabutylammonium perchlorate, CF_3SO_3H and $(CF_3CO)_2O$ in CH_2Cl_2 to form asymmetric arylalkylsulfonium salts (Scheme 9) [68]. The coupling reaction is accompanied by quantitative O_2 uptake; for each mole of O_2 consumed, 2 mol of the product is produced.

The oxidative polymerization of diphenyl disulfide using O_2 as an oxidant can also be catalyzed by $VO(acac)_2$ in the presence of CF_3SO_3H and $(CF_3CO)_2O$ in 1,1,2,2-tetrachloroethane at room temperature to produce oligo(thio-1,4-phenylene) containing one disulfide bond in the chain with the weight-averaged molecular weight of 5450 [2]. The product is obtained as a white, highly pure powder in contrast to the commercially available polymer produced by the high-temperature polycondensation process from *p*-dichlorobenzene and sodium sulfide and contaminated with the eliminated salt. A linear thio-1,4-phenylene structure without any branching or cross-linking has been confirmed by spectroscopy. Further modification of the oligomer has been achieved by the thermolysis or the reductive cleavage of the disulfide bond as a functional group which is mainly located at the end of the chain [2]. The oxovanadium-catalyzed polymerization is also applicable to the synthesis of alkyl-substituted polymers. For example, bis(3,5-dimethylphenyl)disulfide and bis(2,5-dimethylphenyl)disulfide yield poly(thio-2,6-dimethyl-1,4-phenylene) and poly(thio-2,5-dimethyl-1,4-phenylene), respectively. The higher solubility of these

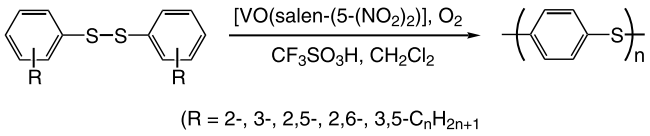

(R = 2-, 3-, 2,5-, 2,6-, 3,5-C_nH_{2n+1}

Scheme 10.

polymers in polymerization solvents such as 1,1,2,2-tetrachloroethane and CH_2Cl_2 results in their higher molecular weights. The polymerization is accompanied by a quantitative O_2 uptake. The kinetics of the polymerization of diphenyl disulfide with $VO(acac)_2$ has been studied based on the rate of O_2 uptake. Lineweaver–Burk plots reveal that the oxidation of diphenyl disulfide is the rate-limiting step. The formation constant of the Michaelis complex K_1 (= reciprocal of the Michaelis constant K_m) and the electron-transfer rate constant k_2 associated with the decomposition of the Michaelis complex has been determined to be $6.3 \times 10\ M^{-1}$ and $6.0 \times 10^{-2}\ min^{-1}$, respectively [2]. A smaller formation constant is obtained with the sterically crowded Michaelis complex produced from bis(2,6-dimethylphenyl)disulfide ($K_1 = 1.4 \times 10\ M^{-1}$, $k_2 = 5.2 \times 10^{-2}\ min^{-1}$) [2]. On the other hand, the O_2-oxidation step of the catalyst becomes the rate-limiting step with monomers more easily oxidized, such as bis(3-methylphenyl)disulfide, bis(3,5-dimethylphenyl)disulfide and bis(2,5-dimethylphenyl)disulfide [2]. A number of oxovanadium(IV) complexes have been found to catalyze the polymerization, such as $[VO(bzac)_2]$, $[VO(tfac)_2]$ and [VO(tpp)]. The catalysis of the reaction by Schiff base complexes has also been found for $[VO(salen–(5\text{-}NO_2)_2)]$ (Scheme 10) [69]. The electrophilic substitution reaction of sulfonium cations formed by the multielectron oxidation of aromatic disulfides or sulfides has been exploited for the synthesis of a variety of poly(thiophenylene) derivatives [70], poly(alkylsulfoniophenylene) salts [71], and ladder-type polyheteroacenes [72] which attract much attention as a new series of functional materials.

The oxidative coupling of 1-methoxynaphthalene in nitrobenzene in the presence of CF_3SO_3H, $(CF_3CO)_2O$ and a catalytic amount of $VO(acac)_2$ under O_2 produced 4,4′-dimethoxy-1,1′-dinaphthyl in high yield; poly(2,5-di-*n*-butoxyphenylene) has also been prepared by oxidative polymerization of 1,4-di-*n*-butoxybenzene catalyzed by $VO(acac)_2$ in 1,2-dichloroethane in the presence of CF_3SO_3H and $(CF_3CO)_2O$ under O_2 [73].

Acknowledgements

Financial support by a Grant-in-Aid for Scientific Research (No. 14703029) from the Ministry of Education, Science, Sports, and Culture in Japan, and Health Science Research Grants (Artificial Blood Project) from the Ministry of Health, Labor and Welfare, Japan is acknowledged.

Appendix A: Abbreviations

Hacac	acetylacetone
Hbzac	benzoylacetone
Htfac	trifluoroacetylacetone
H_2acen	*N*,*N*′-ethylenebis(acetylacetoneimine)
H_2nalphen	bis(2-hydroxy-1-naphthaldehyde)-*o*-phenylenediimine
H_2salen	*N*,*N*′-ethylenebis(salicylideneimine)
H_2salen–(3-EtO)$_2$	*N*,*N*′-ethylenebis(3-ethoxysalicylideneimine)
H_2salen–(5-MeO)$_2$	*N*,*N*′-ethylenebis(5-methoxysalicylideneimine)
H_2salen–(4,6-di-MeO)$_2$	*N*,*N*′-ethylenebis(4,6-di-methoxysalicylideneimine)
H_2salen–(5-Me)$_2$	*N*,*N*′-ethylenebis(5-methylsalicylideneimine)
H_2salen–(3-*tert*-Bu)$_2$	*N*,*N*′-ethylenebis(3-*tert*-butylsalicylideneimine)
H_2salen–(5-(NO$_2$))$_2$	*N*,*N*′-ethylenebis(5-nitrosalicylideneimine)
H_2salen–(3,5-di-*tert*-Bu)$_2$	*N*,*N*′-ethylenebis(3,5-di-*tert*-butylsalicylideneimine)
H_2salen–(3-*tert*-Bu)$_2$–(5-Me)$_2$	*N*,*N*′-ethylenebis(3-*tert*-butyl-5-methylsalicylideneimine)
H_2salphen	*N*,*N*′-*o*-phenylenebis(salicylideneimine)
H_2salphen–(3,5-di-*tert*-Bu)$_2$	*N*,*N*′-*o*-phenylenebis(3,5-di-*tert*-butylsalicylideneimine)
H_2salpn	*N*,*N*′-(1,3-propylene)bis(salicylideneimine)
H_2sal-1,2-pn	*N*,*N*′-(1-methylethylene)bis(salicylideneimine)
H_2sal-(*R*)-pn	*N*,*N*′-disalicylidene-(*R*)-1,2-propanediamine
H_2salptn	*N*,*N*′-(2,2-dimethyl-1,3-propylene)bis(salicylideneimine)
H_2salptn–(3-MeO)$_2$	*N*,*N*′-(2,2-dimethyl-1,3-propylene)bis(3-methoxysalicylideneimine)
H_2salpn–(3-*tert*-Bu)$_2$–(5-Me)$_2$	*N*,*N*′-(1,3-propylene)bis(3-*tert*-butyl-5-methyl-salicylideneimine)
H_2sal-(*R*,*R*)-2,4-ptn–(5-MeO)$_2$	*N*,*N*′-bis(5-methoxysalicylidene)-(*R*,*R*)-2,4-pentanediamine or *N*,*N*′-((*R*,*R*)-1,3-dimethyl-1,3-propylene)bis(5-methoxysalicylideneimine)
H_2sal-(*R*,*R*)-2,4-ptn–(3-EtO)$_2$	*N*,*N*′-bis(3-ethoxysalicylidene)-(*R*,*R*)-2,4-pentanediamine or *N*,*N*′-((*R*,*R*)-1,3-dimethyl-1,3-propylene)bis(3-ethoxysalicylideneimine)

Appendix (*Continued*)

H_2sal–*meso*-stien–(3-EtO)$_2$	*N*,*N*′-bis(3-ethoxysalicylidene-(*R*,*S*)(*S*,*R*)-1,2-diphenyl-1,2-ethanediamine)
H_2salton–(3-EtO)$_2$	*N*,*N*′-bis(3-ethoxysalicylidene-1,2-diphenyl-1,2-ethenediamine)
H_2phepca	*N*-[2-((2-phenolylmethylene)amino)phenyl]pyridine-2-carboxamide
H_2thipca	*N*-[2-((2-thiophenolylmethylene)amino)phenyl]pyridine-2-carboxamide
py	pyridine
H_2tpp	*meso*-tetraphenylporphyrin
Fc	ferrocene

References

[1] (a) S. Iwata, C. Ostermeier, B. Ludwig, H. Michel, Nature 376 (1995) 660;
(b) T. Tsukihara, H. Aoyama, E. Yamashita, T. Tomizaki, H. Yamaguchi, K. Shinzawa-Itoh, R. Nakashima, R. Yaono, S. Yoshikawa, Science 269 (1995) 1069.

[2] (a) E. Tsuchida, K. Yamamoto, M. Jikei, H. Nishide, Macromolecules 22 (1989) 4138;
(b) K. Oyaizu, J. Katoh, F. Suzuki, M. Jikei, K. Yamamoto, H. Nishide, E. Tsuchida, Polym. Adv. Technol. 2 (1991) 155;
(c) K. Yamamoto, E. Tsuchida, H. Nishide, M. Jikei, K. Oyaizu, Macromolecules 26 (1993) 3432;
(d) K. Yamamoto, M. Jikei, K. Oyaizu, F. Suzuki, H. Nishide, E. Tsuchida, Bull. Chem. Soc. Jpn. 67 (1994) 251;
(e) K. Oyaizu, N. Iwasaki, K. Yamamoto, H. Nishide, E. Tsuchida, Bull. Chem. Soc. Jpn. 67 (1994) 1456;
(f) E. Tsuchida, K. Yamamoto, K. Oyaizu, F. Suzuki, H. Nishide, A.S. Hay, Z.Y. Wang, Macromolecules 28 (1995) 409;
(g) K. Yamamoto, K. Oyaizu, E. Tsuchida, Polym. Adv. Technol. 6 (1995) 155;
(h) K. Miyatake, K. Oyaizu, Y. Nishimura, E. Tsuchida, Macromolecules 34 (2001) 1172.

[3] (a) K.S. Patel, G.A. Kolawole, J. Coord. Chem. 15 (1986) 137;
(b) J. Selbin, Chem. Rev. 65 (1965) 153;
(c) J. Selbin, Coord. Chem. Rev. 1 (1966) 293;
(d) M.A. Nawi, T.L. Riechel, Inorg. Chem. 21 (1982) 2268;
(e) M.A. Nawi, T.L. Riechel, Inorg. Chem. 20 (1981) 1974.

[4] K. Oyaizu, K. Yamamoto, K. Yoneda, E. Tsuchida, Inorg. Chem. 35 (1996) 6634.

[5] K. Yamamoto, K. Oyaizu, E. Tsuchida, J. Am. Chem. Soc. 118 (1996) 12665.

[6] E. Tsuchida, K. Oyaizu, E.L. Dewi, T. Imai, F.C. Anson, Inorg. Chem. 38 (1999) 3704.

[7] K. Oyaizu, E. Tsuchida, unpublished results.

[8] (a) K. Oyaizu, E. Tsuchida, J. Am. Chem. Soc. 120 (1998) 237;
(b) K. Oyaizu, K. Yamamoto, Y. Ishii, E. Tsuchida, Chem. Eur. J. 5 (1999) 3193;
(c) H. Nishide, R. Doi, K. Oyaizu, E. Tsuchida, J. Org. Chem. 66 (2001) 1680;
(d) K. Oyaizu, E.L. Dewi, E. Tsuchida, Inorg. Chim. Acta 321 (2001) 205;
(e) A. Haryono, K. Oyaizu, K. Yamamoto, J. Natori, E. Tsuchida, Chem. Lett. (1998) 233;
(f) K. Oyaizu, A. Haryono, H. Yonemaru, E. Tsuchida, J. Chem. Soc. Faraday Trans. 94 (1998) 3393;
(g) K. Oyaizu, A. Haryono, J. Natori, E. Tsuchida, J. Chem. Soc. Faraday Trans. 94 (1998) 3737;
(h) K. Oyaizu, A. Haryono, Y. Nishimura, K. Yamamoto, E. Tsuchida, Bull. Chem. Soc. Jpn. 72 (1999) 1781;
(i) K. Oyaizu, Y. Kumaki, K. Saito, E. Tsuchida, Macromolecules 33 (2000) 5766;
(j) K. Oyaizu, A. Haryono, J. Natori, H. Shinoda, E. Tsuchida, Bull. Chem. Soc. Jpn. 73 (2000) 1151;
(k) K. Oyaizu, T. Nakagawa, E. Tsuchida, Inorg. Chim. Acta 305 (2000) 184;
(l) K. Oyaizu, K. Saito, E. Tsuchida, Chem. Lett. (2000) 1318;
(m) K. Oyaizu, E.L. Dewi, E. Tsuchida, J. Electroanal. Chem. 498 (2001) 136;
(n) K. Oyaizu, A. Haryono, H. Shinoda, E. Tsuchida, Macromol. Chem. Phys. 202 (2001) 1273;
(o) K. Oyaizu, M. Ueno, H. Li, E. Tsuchida, Bull. Chem. Soc. Jpn. 74 (2001) 869.

[9] A. Butler, J.V. Walker, Chem. Rev. 93 (1993) 1937.

[10] M.J. Smith, D. Kim, B. Hornestein, K. Nakanishi, K. Kustin, Acc. Chem. Res. 24 (1991) 117.

[11] R.L. Farmer, F.L. Urbach, Inorg. Chem. 13 (1974) 587.

[12] P.E. Riley, V.L. Pecoraro, C.J. Carrano, J.A. Bonadies, K.N. Raymond, Inorg. Chem. 25 (1986) 154.

[13] K. Oyaizu, E. Tsuchida, unpublished results.

[14] J.R. Zamian, E.R. Dockal, G. Castellano, G. Oliva, Polyhedron 14 (1995) 2411.

[15] C.R. Cornman, K.M. Geiser-Bush, S.P. Rowley, P.D. Boyle, Inorg. Chem. 36 (1997) 6401.

[16] (a) C.V. Grant, K.M. Geiser-Bush, C.R. Cornman, R.D. Britt, Inorg. Chem. 38 (1999) 6285;
(b) C.V. Grant, J.A. Ball, B.J. Hamstra, V.L. Pecoraro, R.D. Britt, J. Phys. Chem. Sect. B 102 (1998) 8145.

[17] J.A. Bonadies, W.M. Butler, V.L. Pecoraro, C.J. Carrano, Inorg. Chem. 26 (1987) 1218.

[18] Z. Liu, F.C. Anson, Inorg. Chem. 39 (2000) 274.

[19] M. Tsuchimoto, G. Hoshina, R. Uemura, K. Nakajima, M. Kojima, S. Ohba, Bull. Chem. Soc. Jpn. 73 (2000) 2317.

[20] M. Pasquali, A. Torres-Filho, C. Floriani, J. Chem. Soc. Chem. Commun. (1975) 534.

[21] M. Pasquali, F. Marchetti, C. Floriani, Inorg. Chem. 18 (1979) 2401.

[22] K.P. Callahan, P.J. Durand, Inorg. Chem. 19 (1980) 3211.

[23] D.L. Hughes, U. Kleinkes, G.J. Leigh, M. Maiwald, J.R. Sanders, C. Sudbrake, J. Weisner, J. Chem. Soc. Dalton Trans. (1993) 3093.

[24] R. Seangprasertkij, T.L. Riechel, Inorg. Chem. 25 (1986) 3121.

[25] R. Seangprasertkij, T.L. Riechel, Inorg. Chem. 23 (1984) 991.

[26] K.P. Callahan, P.J. Durand, Inorg. Chem. 19 (1980) 3211.

[27] D. Bruins, D.L. Weaver, Inorg. Chem. 9 (1970) 130.

[28] M. Sato, K.M. Miller, J.H. Enemark, C.E. Strouse, K.P. Callahan, Inorg. Chem. 20 (1981) 3571.

[29] G. Hoshina, M. Tsuchimoto, S. Ohba, K. Nakajima, H. Uekusa, Y. Ohashi, H. Ishida, M. Kojima, Inorg. Chem. 37 (1998) 142.

[30] J.A. Bonadies, C.J. Carrano, J. Am. Chem. Soc. 108 (1986) 4088.

[31] L. Banci, A. Bencini, A. Dei, D. Gatteschi, Inorg. Chim. Acta 84 (1984) L11.

[32] A.D. Keramidas, A.B. Papaioannou, A. Vlahos, T.A. Kabanos, G. Bonas, A. Makriyannis, C.P. Rapropoulou, A. Terzis, Inorg. Chem. 35 (1996) 357.

[33] M. Pasquali, F. Marchetti, C. Floriani, M. Cesari, Inorg. Chem. 19 (1980) 1198.

[34] N.F. Choudhary, N.G. Connelly, P.B. Hitchcock, G.J. Leigh, J. Chem. Soc. Dalton Trans. (1999) 4437.

[35] S.A. Fairhurst, D.L. Hughes, G.J. Leigh, J.R. Sanders, J. Weisner, J. Chem. Soc. Dalton Trans. (1994) 2591.

[36] K. Oyaizu, E. Tsuchida, unpublished results.
[37] K. Oyaizu, E. Tsuchida, unpublished results.
[38] (a) G.J. Leigh, J.R. Sanders, Polyhedron 8 (1989) 1782;
(b) A. Hills, D.L. Hughes, G.J. Leigh, J.R. Sanders, J. Chem. Soc. Dalton Trans. (1991) 325.
[39] S. Gambarotta, M. Mazzanti, C. Floriani, A. Chiesi-Villa, C. Guastini, J. Chem. Soc. Chem. Commun. (1985) 829.
[40] D. Hall, T.N. Waters, J. Chem. Soc. (1960) 2644.
[41] C.A. Root, J.D. Hoeschele, C.R. Cornman, J.W. Kampf, V.L. Pecoraro, Inorg. Chem. 32 (1993) 3855.
[42] (a) D.L. Hughes, U. Kleinkes, G.J. Leigh, M. Maiwald, J.R. Sanders, C. Sudbrake, J. Chem. Soc. Dalton Trans. (1994) 2457;
(b) A. Hills, D.L. Hughes, G.J. Leigh, J.R. Sanders, J. Chem. Soc. Chem. Commun. (1991) 827.
[43] T.J. Marks, Angew. Chem. Int. Ed. Engl. 29 (1990) 857.
[44] A. Serrette, P.J. Carroll, T.M. Swager, J. Am. Chem. Soc. 114 (1992) 1887.
[45] T.P. Pollagi, T.C. Stoner, R.F. Dallinger, T.M. Gilbert, M.D. Hopkins, J. Am. Chem. Soc. 113 (1991) 703.
[46] I. Aiello, M. Ghedini, F. Neve, D. Pucci, Chem. Mater. 9 (1997) 2107.
[47] M. Mathew, A.J. Carty, G.J. Palenik, J. Am. Chem. Soc. 92 (1970) 3197.
[48] S.A. Fairhurst, D.L. Hughes, U. Kleinkes, G.J. Leigh, J.R. Sanders, J. Weisner, J. Chem. Soc. Dalton Trans. (1995) 321.
[49] A. Hills, D.L. Hughes, G.J. Leigh, J.R. Sanders, J. Chem. Soc. Dalton Trans. (1991) 61.
[50] P.D. Hampton, C.E. Daitch, T.M. Alam, E.A. Pruss, Inorg. Chem. 36 (1997) 2879.
[51] R. Kasahara, M. Tsuchimoto, S. Ohba, K. Nakajima, H. Ishida, M. Kojima, Inorg. Chem. 35 (1996) 7661.
[52] M. Tsuchimoto, R. Kasahara, K. Nakajima, M. Kojima, S. Ohba, Polyhedron 18 (1999) 3035.
[53] H.B. Burgi, Inorg. Chem. 12 (1973) 2321.
[54] Z. Liu, F.C. Anson, Inorg. Chem. 40 (2001) 1329.
[55] E. Tsuchida, K. Yamamoto, K. Oyaizu, N. Iwasaki, F.C. Anson, Inorg. Chem. 33 (1994) 1056.
[56] J.A. Bonadies, V.L. Pecoraro, C.J. Carrano, J. Chem. Soc. Chem. Commun. (1986) 1218.
[57] (a) D.O. Cowan, C.L. Vanda, J. Park, F. Kaufman, Acc. Chem. Res. 6 (1973) 1;
(b) G.C. Allen, N.S. Hush, Prog. Inorg. Chem. 8 (1967) 357;
(c) N.S. Hush, Prog. Inorg. Chem. 8 (1967) 391;
(d) N.S. Hush, Coord. Chem. Rev. 64 (1985) 135.
[58] K. Yamamoto, K. Oyaizu, N. Iwasaki, E. Tsuchida, Chem. Lett. (1993) 1223.
[59] K.P. Callahan, P.J. Durand, Inorg. Chem. 19 (1980) 3217.
[60] A. Jezieski, J.B. Raynor, J. Chem. Soc. Dalton Trans. (1981) 1.
[61] (a) R. Curci, F.D. Furia, R. Testi, G. Modena, J. Chem. Soc. Perkin Trans. 2 (1974) 753;
(b) J.A. Howard, J.C. Tait, T. Yamada, J.H.B. Chenier, Can. J. Chem. 59 (1981) 2184.
[62] J.P. Collman, D.S. Wagenknecht, J.E. Hutchinson, Angew. Chem. Int. Ed. Engl. 33 (1994) 1537.
[63] (a) B. Steiger, C. Shi, F.C. Anson, Inorg. Chem. 32 (1993) 2107;
(b) B. Steiger, F.C. Anson, Inorg. Chem. 33 (1994) 5767.
[64] J.H. Swinehart, Chem. Commun. (1991) 1443.
[65] Y. Sun, B.R. James, S.J. Rettig, C. Orvig, Inorg. Chem. 35 (1996) 1667.
[66] E. Tsuchida, K. Yamamoto, K. Oyaizu, J. Electroanal. Chem. 438 (1997) 167.
[67] N. Toshima, Makromol. Chem. Macromol. Symp. 59 (1992) 123.
[68] K. Yamamoto, S. Kobayashi, E. Shouji, E. Tsuchida, J. Org. Chem. 61 (1996) 1912.
[69] K. Oyaizu, E. Tsuchida, unpublished results.
[70] (a) K. Yamamoto, K. Oyaizu, E. Tsuchida, Chem. Lett. (1993) 1101;
(b) K. Yamamoto, K. Oyaizu, E. Tsuchida, Maromol. Chem. Phys. 195 (1994) 3087;
(c) E. Tsuchida, K. Yamamoto, E. Shouji, A. Haryono, Chem. Commun. (1996) 2091;
(d) K. Miyatake, H. Iyotani, K. Yamamoto, E. Tsuchida, Macromolecules 29 (1996) 6969;
(e) K. Miyatake, E. Shouji, K. Yamamoto, E. Tsuchida, Macromolecules 30 (1997) 2941;
(f) K. Miyatake, Y. Yokoi, K. Yamamoto, E. Tsuchida, A.S. Hay, Macromolecules 30 (1997) 4502;
(g) K. Yamamoto, K. Oyaizu, S. Kobayashi, E. Tsuchida, Phosphorus Sulfur Silicon Relat. Elem. 120–121 (1997) 407;
(h) K. Miyatake, K. Yamamoto, Y. Yokoi, E. Tsuchida, Macromolecules 31 (1998) 403;
(i) E. Tsuchida, K. Miyatake, K. Yamamoto, A.S. Hay, Macromolecules 31 (1998) 6469;
(j) Y. Ding, A.R. Hlil, A.S. Hay, E. Tsuchida, K. Miyatake, Macromolecules 32 (1999) 315;
(k) K. Miyatake, H. Hara, E. Tsuchida, Macromol. Chem. Phys. 200 (1999) 1930;
(l) K. Miyatake, J.-S. Cho, S. Takeoka, E. Tsuchida, Macromol. Chem. Phys. 200 (1999) 2897;
(m) K. Miyatake, K. Endo, E. Tsuchida, Macromolecules 32 (1999) 8786;
(n) K. Miyatake, K. Fukushima, S. Takeoka, E. Tsuchida, Chem. Mater. 11 (1999) 1171;
(o) J.-S. Cho, Y. Hayashino, K. Miyatake, S. Takeoka, E. Tsuchida, Polym. Adv. Technol. 11 (2000) 548.
[71] (a) E. Tsuchida, K. Yamamoto, K. Miyatake, Y. Nishimura, Angew. Chem. Int. Ed. Engl. 35 (1996) 2843;
(b) K. Miyatake, A. Haryono, K. Oyaizu, E. Tsuchida, J. Macromol. Sci. Sect. A 38 (2001) 851;
(c) K. Oyaizu, Y. Ikai, E. Tsuchida, J. Macromol. Sci. Sect. A 38 (2001) 1049;
(d) K. Yamamoto, K. Miyatake, Y. Nishimura, E. Tsuchida, Chem. Commun. (1996) 2099;
(e) A. Haryono, K. Yamamoto, E. Shouji, E. Tsuchida, Macromolecules 31 (1998) 1202;
(f) E. Tsuchida, K. Miyatake, Chin. J. Polym. Sci. 16 (1998) 106;
(g) K. Miyatake, K. Yamamoto, K. Endo, E. Tsuchida, J. Org. Chem. 63 (1998) 7522;
(h) K. Miyatake, T. Ishikawa, E. Tsuchida, Macromolecules 32 (1999) 4497;
(i) A. Haryono, K. Miyatake, E. Tsuchida, Macromol. Chem. Phys. 200 (1999) 1257;
(j) K. Oyaizu, H. Nakano, J. Natori, E. Tsuchida, J. Electroanal. Chem. 498 (2001) 232.
[72] (a) A. Haryono, K. Miyatake, J. Natori, E. Tsuchida, Macromolecules 32 (1999) 3146;
(b) K. Miyatake, A.S. Hay, F. Mitsuhashi, E. Tsuchida, Macromolecules 34 (2001) 2385.
[73] T. Okada, T. Ogata, M. Ueda, Macromolecules 29 (1996) 7645.